

Low Temperature CO Oxidation over Unsupported Nanoporous Gold

Caixia Xu,[†] Jixin Su,[‡] Xiaohong Xu,[†] Pengpeng Liu,[†] Hongjuan Zhao,[†] Fang Tian,[†] and Yi Ding^{*,†}

Key Laboratory of Colloid and Interface Chemistry, Ministry of Education, School of Chemistry and Chemical Engineering, and School of Environmental Science and Engineering, Shandong University, Jinan 250100, China

Received October 22, 2006; E-mail: yding@sdu.edu.cn

Nanostructured gold, when prepared in a certain manner, exhibits high activity in both heterogeneous and homogeneous catalysis,^{1–3} such as CO oxidation, NO reduction, oxidation of hydrocarbons, etc. Among them, CO oxidation over supported gold nanoparticles has been most extensively investigated.^{4–8} In particular, the role of catalyst support is a topic of continuous debate, and different mechanisms have been proposed.⁹ The controversy mainly stems from the fact that the supported gold catalyst is a composite system, and its apparent catalytic activity is a result of interplay among many factors, including particle size, preparation method, choice of support, pretreatment conditions, etc. In this paper, we report that significant CO oxidation reactivity can be obtained over unsupported nanoporous gold (NPG). By completely excluding the support effect, this research takes one step further toward understanding the origin of the exceptional catalytic behavior of gold.

NPG is made by selective dissolution (dealloying) of silver from silver/gold alloy.¹⁰ In previous work, we have shown that etching white gold leaf in nitric acid generates a free-standing nanoporous gold membrane material with controllable three-dimensional porosity.¹¹ However, under similar free corrosion conditions, dealloying a bulk Ag/Au foil requires extended time, which results in a coarsened structure (Figure 1a) due to the fast diffusion of gold in electrolyte.^{11a} For catalysis, a higher surface area material is needed, and enhanced activity is often observed when gold nanoparticles have a size less than 10 nm.¹ Because the dealloying process is a competition between dissolution induced surface roughening and diffusion induced surface smoothing,^{10b} we employed a modified dealloying by etching Ag/Au in concentrated nitric acid under applied anodic potential. In this way, bulk nanoporous gold can be routinely fabricated with ligament sizes less than 6 nm (Figure 1b and Figure S1).

The catalytic activity of NPG was measured with a continuous flow fixed-bed microreactor. Figure 2 shows the catalytic performance of NPG for CO oxidation at different temperatures. It was found that unsupported NPG could maintain a CO conversion rate higher than 99.5% for nearly 20 h at room temperature, after which the catalytic efficiency gradually decreased, and the conversion dropped to ~75% after 35 h. It is known that supported gold exhibits low-temperature catalytic properties, and we indeed found that significant activities (>85% conversion) could be achieved at low temperatures, such as –30 °C (black curve), and no apparent activity loss was found in 30 h. The deactivation of the Au catalyst has also been observed in other systems,^{4,6b} which is usually caused by cluster aggregation. The insets of Figure 2 show the SEM images of NPG samples after catalytic reactions. Compared to Figure 1b, the ligament size dramatically increased to around ~20 nm for the room temperature sample, and clogging of pores could be observed in some areas. The coarsening of the porous structure reduced the active surface area, which eventually led to reduced activity. In

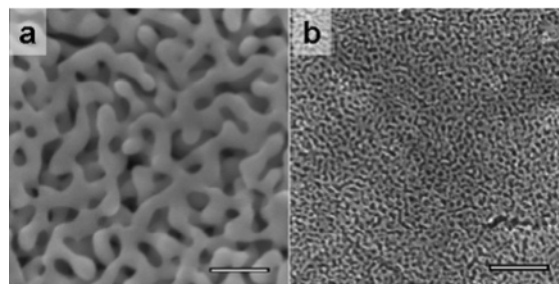


Figure 1. SEM images of NPG samples. (a) *f*-NPG dealloyed at room temperature (rt) for 128 min in nitric acid under free corrosion conditions; (b) *a*-NPG dealloyed at rt for 15 min in nitric acid with an anodic potential of 1.0 V. Scale bars: 100 nm.

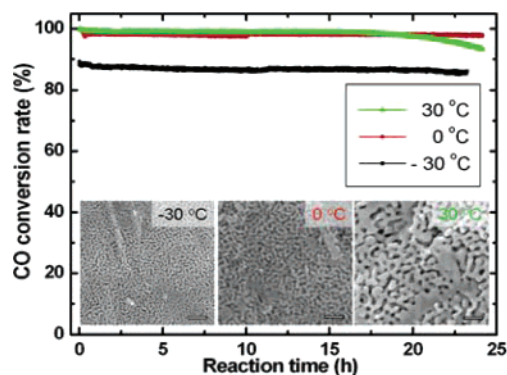


Figure 2. Catalytic performance of *a*-NPG at different temperatures. In each experiment, 50 mg of NPG catalyst and a gas mixture of 1% CO, 10% O₂, and 89% N₂ were used with a flow rate of 66.7 mL/min, corresponding to a space velocity of 80 040 mL/h *g*_{cat}⁻¹. The turnover frequency (TOF) was measured to be about 0.034 s⁻¹. Insets are SEM images of NPG samples after catalytic reactions. Scale bars: 100 nm.

contrast, the structure coarsening was significantly retarded at lower temperatures, and catalytic reaction at –30 °C for over 30 h increased the pore size from the original 5 to ~8 nm. This property offers the NPG catalyst a unique advantage of performing at low temperatures with sustained stability.

It is worth mentioning that all NPG samples were tested as made without any activation pretreatment. This is in sharp contrast to most supported Au catalysts which require preactivation in H₂ and/or O₂ flow at elevated temperatures in order to gain sufficient activity.^{1,6b} We note that nanoparticulate Au catalysts are usually made through wet-chemistry method (impregnation, co-precipitation or deposition–precipitation) from auric solutions, such as HAuCl₄, thus activation is essential in order to expose surface active sites by removing protectors, chloride ions, etc. However, NPG is made with an absolutely different process, and porous structures are generated from etching high purity alloys in HNO₃, which results in a very clean surface as confirmed by HRTEM observations.^{11a}

Previous studies have reported that both ionic and neutral gold clusters exhibit enhanced catalytic activities;^{1,5,12} it is thus necessary

[†] School of Chemistry and Chemical Engineering.

[‡] School of Environmental Science and Engineering.

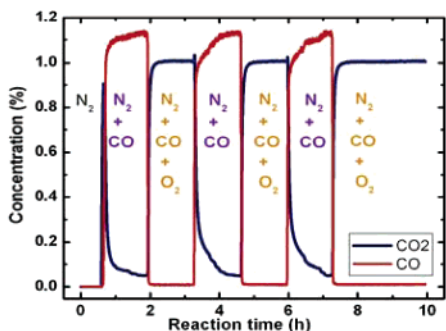


Figure 3. Catalyst performance of 50 mg of *a*-NPG under different testing conditions. (I) N₂ gas, flow rate = 60 mL/min, 30 min; (II) 1.11% CO/N₂ mixed gas, flow rate = 60 mL/min, 80 min for each step; (III) 1% CO/10% O₂/N₂ mixed gas, flow rate = 66.7 mL/min, 80 min for each step.

to study the surface state of NPG in order to gain better insight into the origin of its catalytic properties. Because NPG used in this experiment is made through anodic etching in HNO₃ with a potential high enough to oxidize gold, X-ray photoelectron spectroscopy (XPS) was used to study the chemical state of NPG (see Supporting Information). Analysis of the core-level XPS spectra of both anodic-etched (*a*) and free-corroded (*f*) NPG shows that *f*-NPG is metallic in state (4f binding energies of 83.9 and 87.6 eV), whereas *a*-NPG clearly has gold oxides¹³ on the surface (4f binding energies of 85.5 and 89.1 eV). The existence of gold oxides was further confirmed by electrochemical linear scan voltammetry (LSV) in dilute sulfuric acid. The current–potential curves were recorded by scanning from an open circuit potential of 1.06 V (vs SCE for *a*-NPG) to 0 V. While 1.06 V is not high enough to oxidize Au, we clearly see a dominant cathodic peak around 0.7 V (Figure S4), corresponding to the reduction of gold oxide on NPG. In contrast, the electrochemical behavior of *f*-NPG in this potential range is featureless, indicative of its pure elemental state, which is also consistent with the XPS analysis. It has to be emphasized that, although in our sample oxidized gold exists in an appreciable amount, gold oxide itself is less likely working as a catalyst for CO oxidation. This is supported by two observations: (1) *f*-NPG also shows appreciable catalytic activity in this reaction (Figure S6); (2) gold oxide on *a*-NPG quickly disappears upon CO gas feeding. The red curve in Figure S4 shows the LSV behavior of an *a*-NPG sample which has been subject to CO oxidation at room temperature for 10 h, at which the conversion rate was still close to 100%. However, no gold oxides were detected. This strongly suggests that it is metallic gold that is playing the catalytic role in this reaction.

We also explored the catalytic behavior of *a*-NPG under various experimental conditions. In a typical experiment (shown in Figure 3), pure N₂ gas was first fed into the microreactor loaded with 50 mg of *a*-NPG catalyst. In this period, neither CO nor CO₂ was detected. After 40 min, CO/N₂ mixed gas was introduced into the system, and we saw a sharp increase to over 0.8% in CO₂ concentration followed by a rapid decrease to less than 0.05% as detected with an on-line gas analyzer. Because we did not feed O₂, the appearance of CO₂ in the product is solely due to the redox reaction of CO with surface gold oxides in the sample. In comparison, the CO signal has a short delay and then continues with a dramatic increase to its original concentration of 1.11% in the mixed gas as gold oxides were gradually depleted within the sample. The operation was continued by introducing O₂ into the system, and the CO conversion rapidly increases to ~100% and holds due to the catalytic activity of the metallic state of nanoporous gold. After an additional 80 min, O₂ feeding was turned off, and we saw that CO₂ concentration immediately declined. It is noted

that CO₂ concentration will not achieve zero. This is not due to any residual gold oxides in the sample. In fact, gas chromatography analysis confirms that there is a slight amount of O₂ (0.02%) in the CO/N₂ mixed gas (Figure S7). Similar operations have been repeated three times, and each time, NPG could resume an activity of nearly 100%. This further demonstrates NPG's remarkable catalytic stability and tolerance to CO poisoning.

In summary, NPG with sub-10 nm pore size has been fabricated with a simple dealloying method. As a novel unsupported catalyst, NPG shows extraordinary properties for various catalytic reactions, and CO oxidation is just the first example. Ongoing research includes optimizing NPG's performance and applying NPG to catalyze other important reactions, such as NO reduction, alcohol and sugar oxidation, methanol electro-carbonylation, etc. Possible contributions from residual Ag atoms (Figure S2) buried within the structure will also be investigated.¹⁴ It is noteworthy that, although our results unambiguously prove that Au's surprising catalytic activity could solely come from nanostructured gold itself, this research would never exclude the possibility that catalyst support could also contribute to enhancing the catalyst performance by, for example, suppressing catalyst sintering,⁴ charge transferring,⁸ or improving the selectivity.¹ Further research is still needed to optimize and correlate NPG's structure and performance, which we believe will greatly deepen our understanding of the remarkable catalytic properties of gold and supported gold catalysts.

Acknowledgment. Financial support from the National Science Foundation of China (NSFC 50601015), the National 863 Program Project (2006AA03Z222), and the 973 Program Project of China (2005CB623601) is greatly appreciated. Y.D. is a Tai-Shan Scholar supported by Shandong Province.

Supporting Information Available: Detailed experimental procedure, optical images of NPG samples, EDS analysis, XPS spectra, LSV curves, GC result, and Figures S1–S7. This material is available free of charge via the Internet at <http://pubs.acs.org>.

References

- Bond, G. C.; Thompson, D. T. *Catal. Rev. Sci. Eng.* **1999**, *41*, 319–388.
- Stephen, A.; Hashmi, K. *Gold Bull.* **2004**, *37*, 51–65.
- (a) Haruta, M. *Catal. Today* **1997**, *36*, 153–166. (b) Haruta, M.; Kobayashi, T.; Sano, H.; Yamada, N. *Chem. Lett.* **1987**, *16*, 405–408.
- Valden, M.; Lai, X.; Goodman, D. W. *Science* **1998**, *281*, 1647–1650.
- (a) Remedakis, I. N.; Lopez, N.; Norskov, J. K. *Angew. Chem., Int. Ed.* **2005**, *44*, 1824–1826. (b) Lopez, N.; Norskov, J. K. *J. Am. Chem. Soc.* **2002**, *124*, 11262–11263.
- (a) Comotti, M.; Li, W. C.; Spliethoff, B.; Schüth, F. *J. Am. Chem. Soc.* **2006**, *128*, 917–924. (b) Comotti, M.; Pina, C. D.; Matarrese, R.; Rossi, M. *Angew. Chem., Int. Ed.* **2004**, *43*, 5812–5815.
- Wallace, W. T.; Whetten, R. L. *J. Am. Chem. Soc.* **2002**, *124*, 7499–7505.
- Arrii, S.; Morfin, F.; Renouprez, A. J.; Rousset, J. L. *J. Am. Chem. Soc.* **2004**, *126*, 1199–1205.
- Sanchez-Castillo, M. A.; Couto, C.; Kim, W. B.; Dumesic, J. A. *Angew. Chem., Int. Ed.* **2004**, *43*, 1140–1142.
- (a) Newman, R. C.; Sieradzki, K. *Science* **1994**, *263*, 1708–1709. (b) Erlebacher, J.; Aziz, M. J.; Karma, A.; Dimitrov, N.; Sieradzki, K. *Nature* **2001**, *410*, 450–453.
- (a) Ding, Y.; Kim, Y. J.; Erlebacher, J. *Adv. Mater.* **2004**, *16*, 1897–1900. (b) Ding, Y.; Erlebacher, J. *J. Am. Chem. Soc.* **2003**, *125*, 7772–7773. (c) Ding, Y.; Chen, M. W.; Erlebacher, J. *J. Am. Chem. Soc.* **2004**, *126*, 6876–6877.
- Fu, L.; Wu, N. Q.; Yang, J. H.; Qu, F.; Johnson, D.; Kung, C.; Kung, H. H.; Dravid, V. P. *J. Phys. Chem. B* **2005**, *109*, 3704–3706.
- Boyen, H. G.; Kastle, G.; Weig, F.; Koslowski, B.; Dietrich, C.; Ziemann, P.; Spatz, J. P.; Riethmüller, S.; Hartmann, C.; Moller, M.; Schmid, G.; Garnier, M. G.; Oelhafen, P. *Science* **2002**, *297*, 1533–1536.
- Liu, J. H.; Wang, A. Q.; Chi, Y. S.; Lin, H. P.; Mou, C. Y. *J. Phys. Chem. B* **2005**, *109*, 40–43.

JA0675503